The EMBO Journal vol.5 no.3 pp.519–528, 1986

Cryo-electron microscopy of vitrified SV40 minichromosomes: the liquid drop model

Jacques Dubochet, Marc Adrian, Patrick Schultz[1] and Pierre Oudet[1]

European Molecular Biology Laboratory (EMBL), Postfach 10.2209, D-6900 Heidelberg, FRG, and [1]Institut de Chimie Biologique, 11 rue Humann, 6700 Strasbourg, France

Communicated by J.E.Edstrom

The structure of SV40 minichromosomes has been studied by cryo-electron microscopy of vitrified thin layers of solution. In high-salt buffer (130 mM NaCl), freshly prepared minichromosomes are condensed into globules 30 nm or more in diameter. On the micrograph, they appear to be formed by the close packing of 10 nm granules which give rise to a 10 nm reflection in the optical diffractogram. The globules can adopt many different conformations. At high concentration, they fuse into a homogeneous 'sea' of closely packed 10 nm granules. In low-salt buffer (< 10 mM NaCl), the globules open, first into 10 nm filaments, and then into nucleosome-strings. The 'liquid drop' model is proposed to explain the condensed structure of the minichromosome in high-salt buffer: nucleosomes stack specifically on top of one another, thus forming the 10 nm filaments. 10 nm filaments in turn, tend to aggregate laterally. Optimizing both these interactions results in the condensation of 10 nm filaments or portions thereof into a structure similar to that of a liquid. Some implications of this model for the structure of cellular chromatin are discussed.

Key words: minichromosomes/SV40/cryo-electron microscopy/liquid drop model

Introduction

The 1.6 μm long, double-stranded circular genome of the Simian virus SV40 is replicated in the nucleus of infected mammalian cells and together with the viral proteins, cellular histones and some other cellular proteins, is assembled into a complete virion (reviewed in Tooze, 1982). One well-defined assembly complex can be isolated during virus synthesis (Keller *et al.*, 1977). It contains one DNA molecule, all five histones, including H1, and viral proteins, in particular the capsid protein V1. On a sucrose gradient, it forms a peak at 75S, well separated from the virus which sediments at 200S. The complex has been termed a 'minichromosome' (Griffiths, 1975) because it exhibits many properties of cellular chromatin. In particular, the histone-DNA association takes the form of 20–25 nucleosomes similar to those of the cell. Many reports have shown that the nucleosome string can be further condensed into higher-order structures, such as 40 nm globules (Keller *et al.*, 1977; Varshavsky *et al.*, 1978), or filaments 10 nm in diameter (Griffiths, 1975). In contrast to cellular chromatin, the minichromosome can be isolated under physiological salt conditions. For all these reasons, the minichromosome is frequently considered to be an excellent model with which to investigate chromation structure and function, and the way nucleosomes are packed into higher-order structures. This approach must, however, be considered with care because as the name minichromosome indicates, it emphasizes the similarity of the model with chromosomes but neglects its relation with the virus itself. In particular, the role of the minichromosome in virus ontogeny has not been studied specifically and the effect of the viral proteins on minichromosome structure is also unknown.

Most conventional electron microscopical observations of higher-order structures in chromatin and in the minichromsome are difficult to reproduce, and the images obtained are inadequate for detailed structural analysis. This is probably due to the inherent limitations of conventional preparation procedures. The newly developed technique of cryo-electron microscopy of vitrified suspensions avoids the usual preparation artefacts (Adrian *et al.*, 1984). It allows specimens to be observed with their full water content, in a defined ionic environment, and without suffering from ice crystal formation. The method is best applied to unfixed, unstained and unsupported thin layers of suspension. We report here on observations made using this method with minichromosome suspensions.

Results

A typical SDS gel analysis of minichromosome proteins is shown in Figure 1a. As observed previously, all histones, including H1,

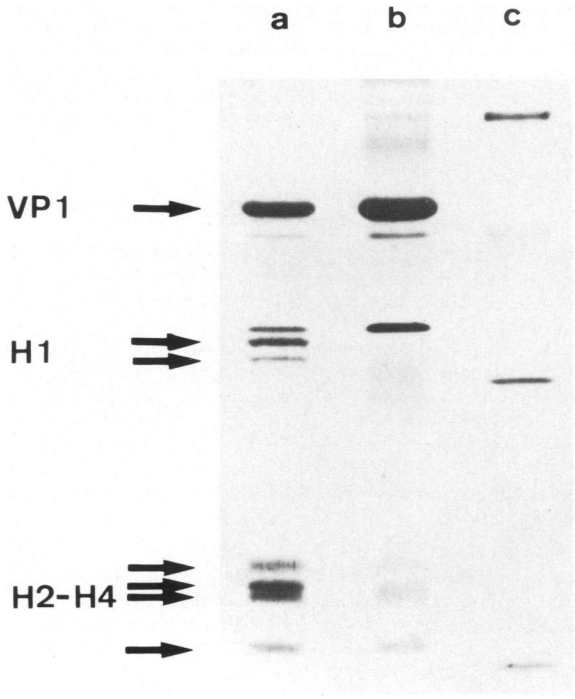

Fig. 1. SDS gels of proteins from (**a**) fresh minichromosomes isolated and purified in high-salt buffer containing 130 mM NaCl (Varshavsky *et al.*, 1977), (**b**) purified viruses, and (**c**) mol. wt standards (Pharmacia, Uppsala, Sweden) of 68,43,30 and 14 Kd.

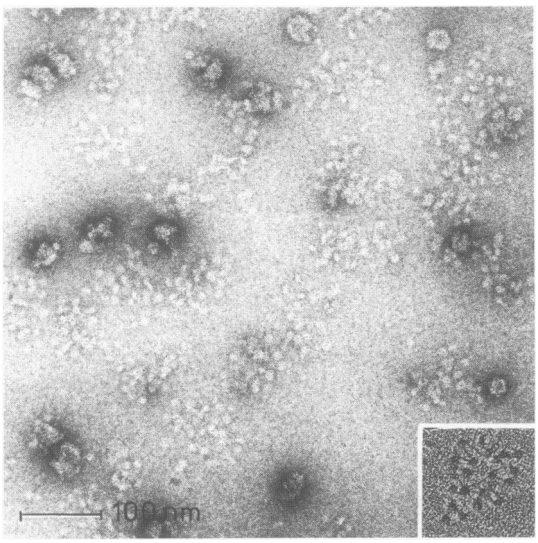

Fig. 2. Fresh solution of SV40 minichromosome (50 μg DNA/ml, high-salt buffer with 50 mM NaCl) mounted on a hydrophilic carbon film and negatively stained with 2% uranyl acetate. Insert: Same solution mounted on positively charged carbon film, stained and shadowed as described previously (Oudet *et al.*, 1975). Magnification 140 000×.

and the viral proteins VP1, 2 and 3 are present (Keller *et al.*, 1977). As previously described (reviewed in Tooze, 1982), the ratio of H1 to the four other histones is the same as for cellular chromatin: one H1 molecule for eight other histones. In comparison, the purified virus is mostly made of viral proteins. It contains no H1 (Figure 1b). An agarose gel electrophoresis analysis of the deproteinized DNA shows that nearly all the DNA is supercoiled (not shown). When observed with conventional electron microscopical methods, the fresh minichromosomes have the same appearance as in previous studies (reviewed in Tooze, 1982). Negative staining on a hydrophilic support (Keller *et al.*, 1977) shows groups of 20–25 nucleosomes and irregular globules of ~40 nm diameter (Figure 2). Adsorption and staining of minichromosomes on a positively-charged support (Dubochet *et al.*, 1971) produces the well-known nucleosome zig-zag (Figure 2, insert).

The dominant features in vitrified, unstained thin layers of fresh minichromosome solutions in 50–130 mM NaCl are globules which, by optical diffraction, give a characteristic ring at $(10.3 \pm 0.5\ \text{nm})^{-1}$. Two examples are shown in Figure 3. Figure 4 also shows the unmistakable difference between the globule and the virus or virus capsid: when a preparation of globules (a), is mixed with a purified virus solution (b), both

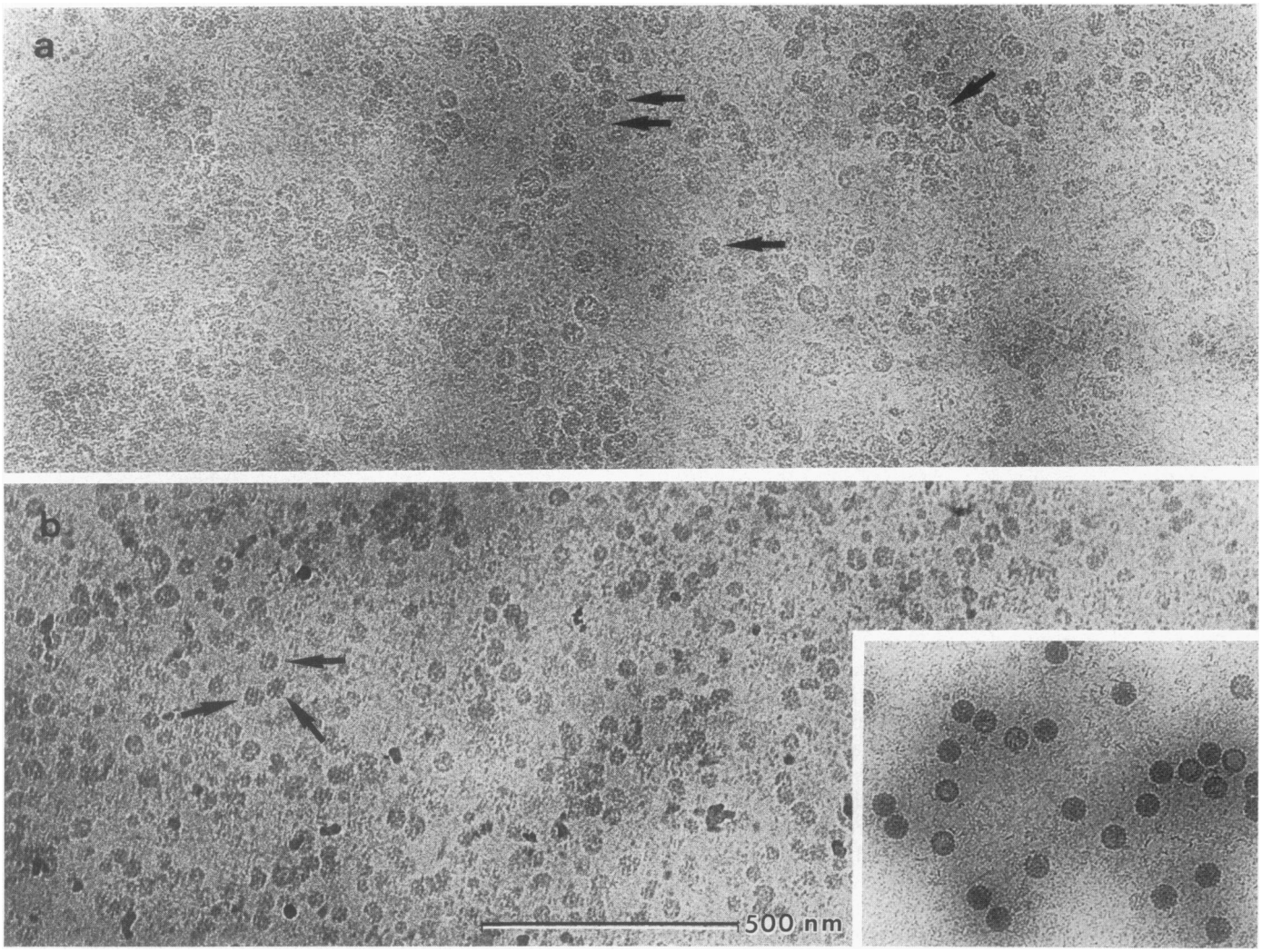

Fig. 3. Thin (~100 nm) vitrified layer of unstained, unfixed and unsupported fresh minichromosome solution (50 μg DNA/ml, 50 mM NaCl). Black arrows indicate globules where the 10 nm granularity is clearly visible. Insert: thin vitrified layer of unstained, unfixed and unsupported SV40 solution. Magnification: 75 000×.

types of particles are still clearly discernible in the mixed preparation (c). Within any given preparation the size and shape of the globules are always variable. A histogram of the diameter of the rounded globules is presented in Figure 5. For comparison, the size distribution of the purified virus particles is also shown. In addition, some globular, or open minichromosomes are visible in the background of most fresh preparations. At very high concentration, individual globules are indistinguishable. Instead, the

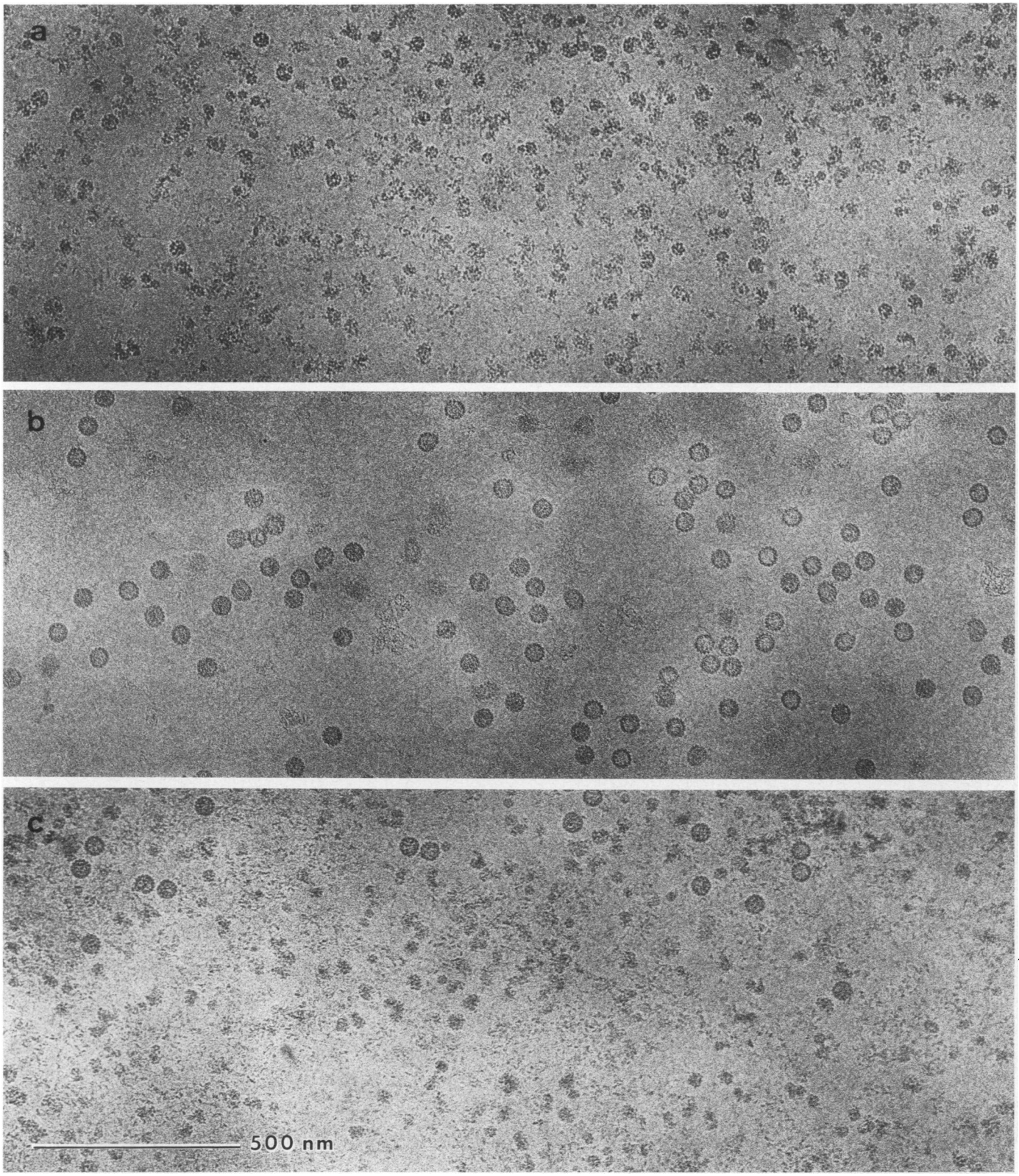

Fig. 4. Minichromosome (**a**), purified virus particles (**b**) and mixture of both (**c**) observed under identical conditions. The three samples are in the high-salt buffer with 130 mM NaCl. The minichromosomes are at a concentration corresponding to 50 μg DNA/ml. The virus concentration is 200 μg/ml. The mixture contains 5 vol of minichromosome solution and 1 vol of virus solution. They are prepared for electron microscopy as in Figure 3. Magnification: 75 000×.

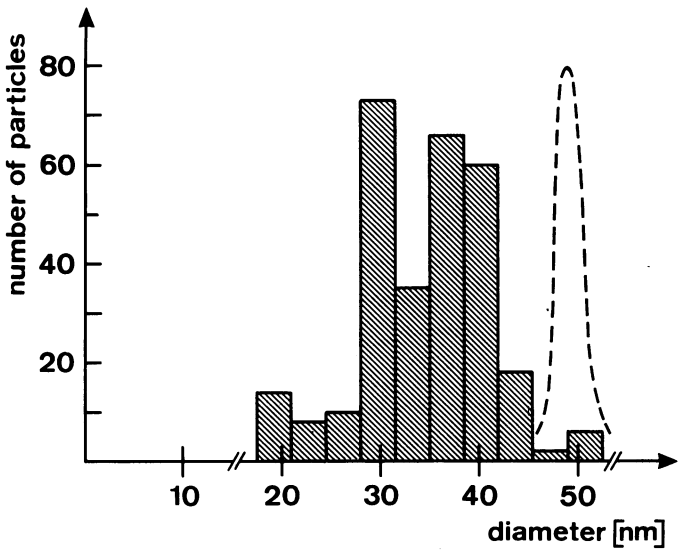

Fig. 5. Histogram of the diameter of the globules observed in three different preparations included those from which Figure 3a and b were derived. Only rounded globules were measured. The bimodal aspect of the distribution was apparent in each of the three preparations. The size distribution of purified virus particles is shown with a dashed line for comparison.

image displays a homogeneous granularity, also giving rise to the 10 nm ring in the optical diffractogram (Figure 6).

Morphological features, allowing a more precise characterization of the globules, are seen in most preparations. In some cases, many of the small globules appear as perforated cylinders with an external and an internal diameter of 30 nm and 8 nm respectively (Figure 7a, black arrows). More frequently, the globules appear as complex aggregates of 10 nm granules. This granularity is most clearly visible at the edge of the globules (Figures 3a and 7b, black arrows). At high magnification, many of the smallest globules seem to be made of a discrete number of closely packed 10 nm granules (Figure 7b, white arrows, and Figure 8a). Rows of three to five regularly arranged 10 nm granules are frequently seen at the periphery of larger globules (Figure 7b, black arrows and Figure 8b). In favourable cases, each granule is seen as a 10 nm ring with a ~3 nm low density region in the centre (Figure 7b, Figure 8a and b). Another characteristic but infrequent shape of the small globule is shown in Figure 8c. It is a striated annulus of 25 nm diameter. Eight to eleven striations can generally be counted along the circumference. The centre is generally occupied by one 10 nm granule.

The gloubles open and dissociate within a few days in the 50 nm or 130 nm buffer and within less than one hour when the salt concentration is reduced to 10 mM NaCl or less. This loss

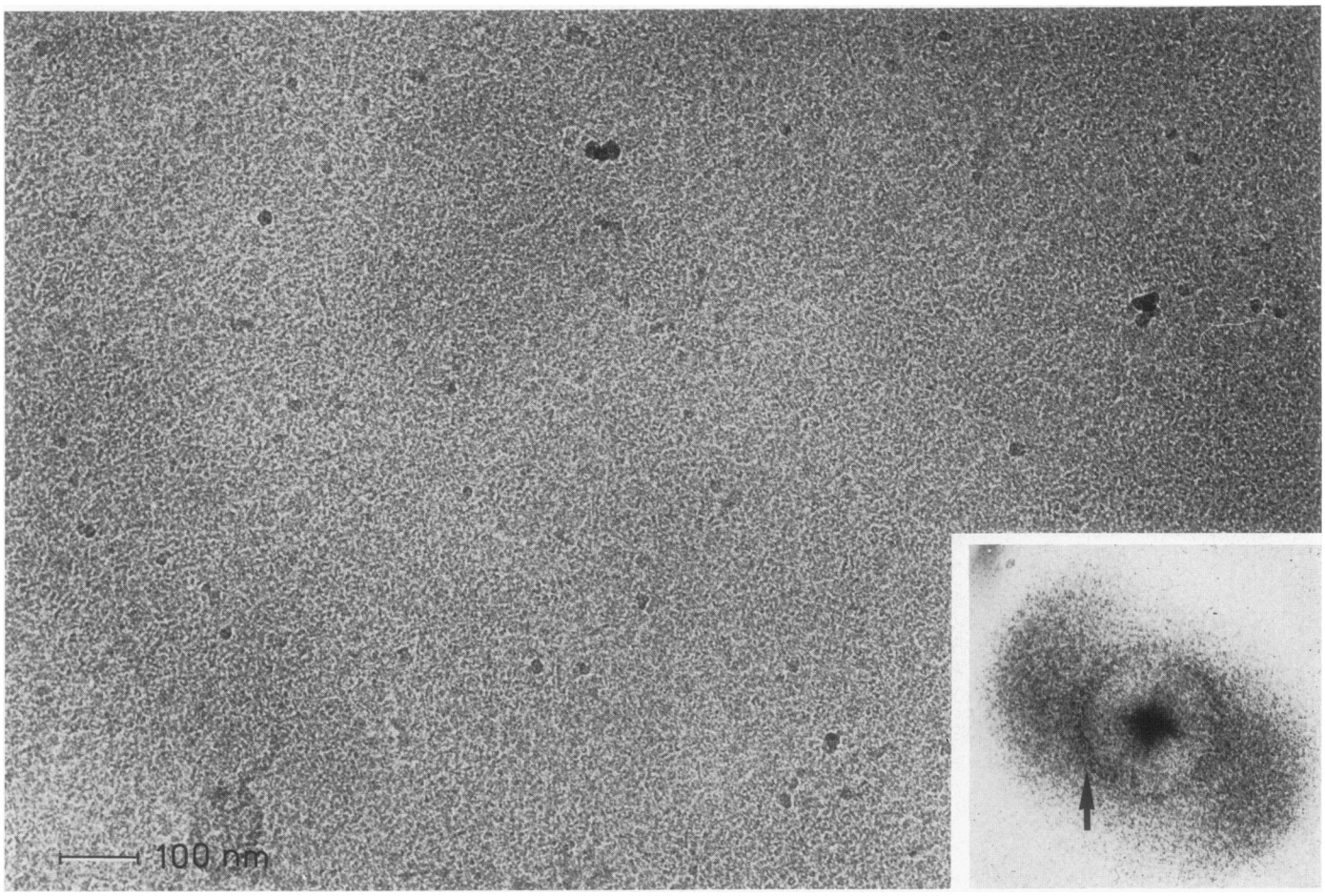

Fig. 6. Vitrified layer of concentrated minichromosome solution in 50 mM NaCl. In this case the 1 mg DNA/ml solution was further concentrated by a process taking place on the bare grid, in the liquid film just prior to vitrification: the minichromosome globules are pushed away from the central region of the grid square where the film thickness is of the order of, or smaller than, the globule diameter. The area shown is at the edge of the concentrated region, where the thickness has the minimum value compatible with the presence of globules. Magnification: 106 000×. Insert: Optical diffractogram corresponding to a 2 μm region of the specimen. The ring marked by an arrow corresponds to a spacing of 10 nm.

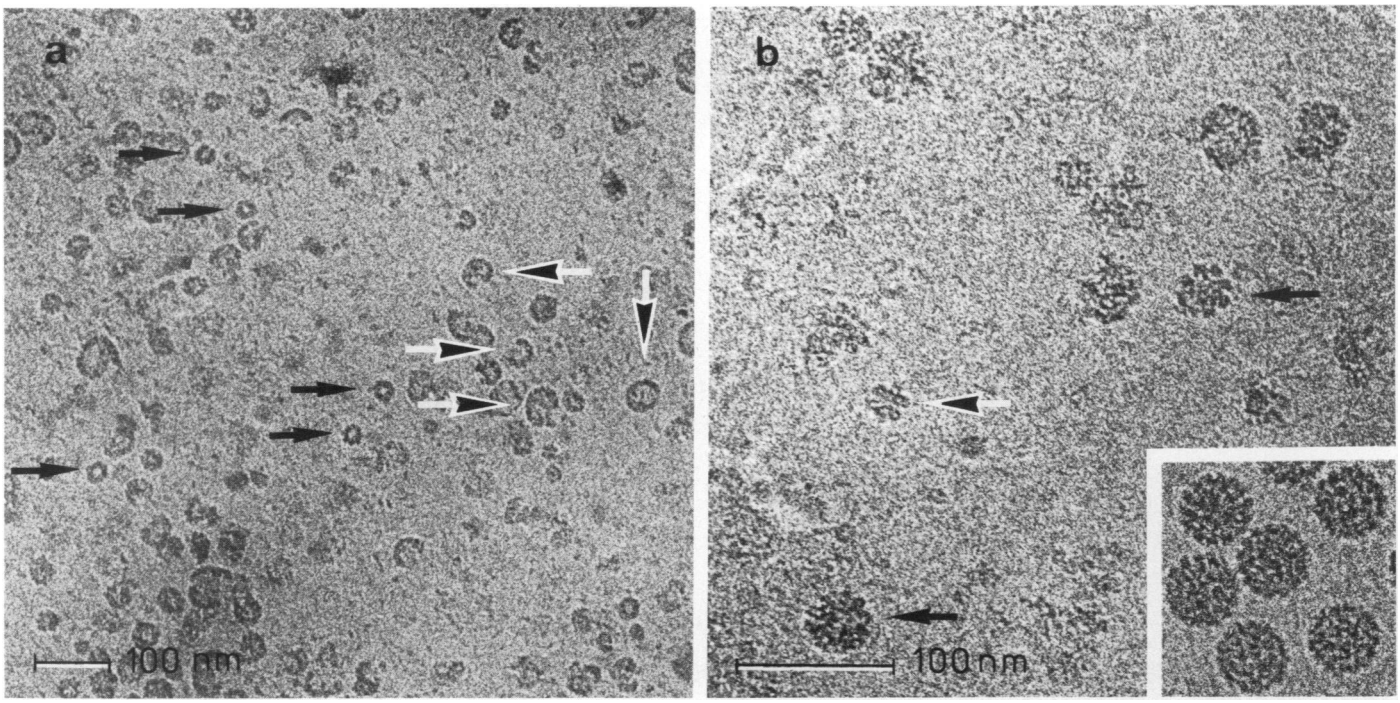

Fig. 7. Two different preparations of fresh minichromosome solution (50 μg DNA/ml). (**a**) Specimen prepared 4 min after the salt concentration was reduced from 50 to 10 mM NaCl. Many globules are still compact and have the characteristic appearance of hollow cylinders (black arrows). The low salt medium has already increased the proportion of partially open globules (white arrows). Magnification: 95 000×. (**b**) Fresh preparation in 50 mM NaCl. Black arrows: 10 nm granules at the edge of the globule. White arrow: globule made by ordered packing of 10 nm granules. Virus particles are shown in insert for comparison. Magnification: 212 000×.

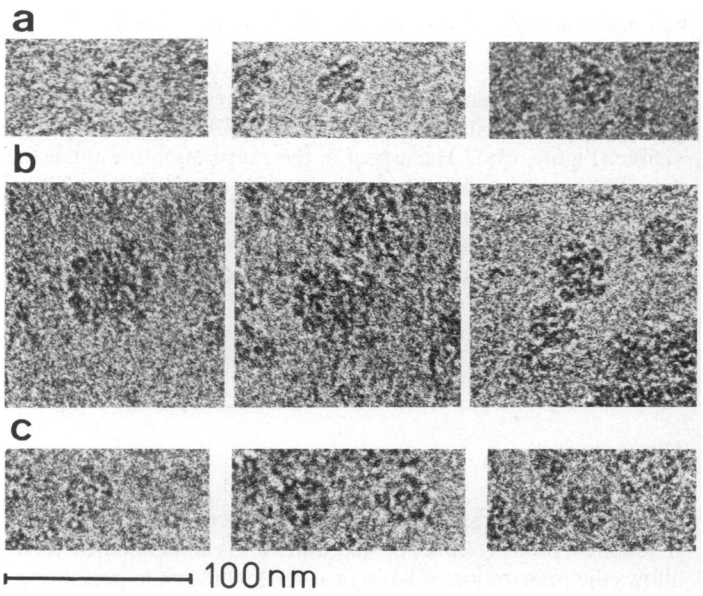

Fig. 8. Morphology of globules. (**a**) The smallest globules are frequently made by the ordered packing of 10 nm granules. (**b**) Regular close packing of 10 nm granules at the surface of the globule. (**c**) Annulus-shaped globules. Magnification: 250 000×.

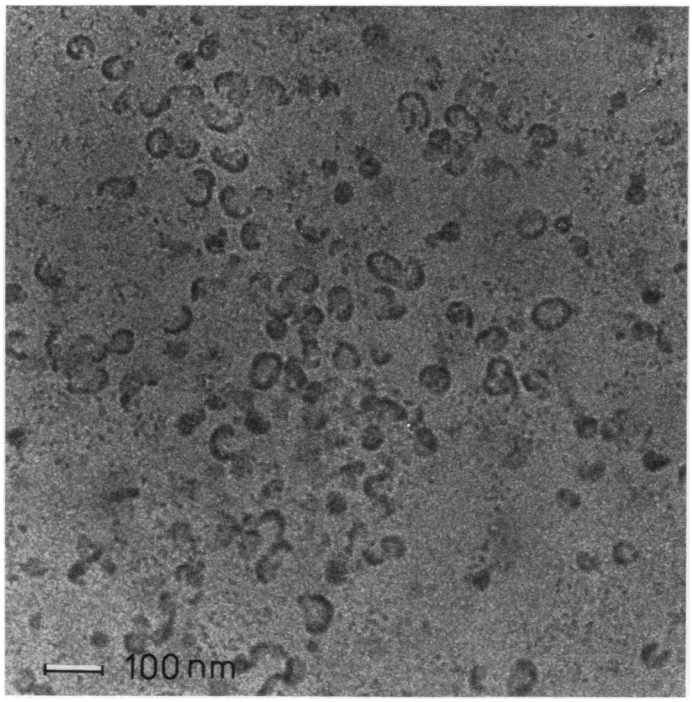

Fig. 9. Minichromosome solution (50 μg DNA/ml) after 10 min in 10 mM NaCl. Most of the globules have opened into 10 nm filaments. Magnification: 75 000×.

of structure is not due to protein loss or degradation since the protein pattern, as tested by SDS gel electrophoresis, is unchanged. In the intermediate state of dissociation, the globules open into curved filaments, 10 ± 2 nm wide. Although some of these filaments are usually visible in fresh 50 mM preparations, they are considerably more numerous shortly after reduction of the salt concentration. In some cases, nearly all the material is in the form of 10 nm filaments (Figure 9). The filaments have an average radius of curvature of approximately 30 nm. They are not all the same length. This may reflect a partial dissociation

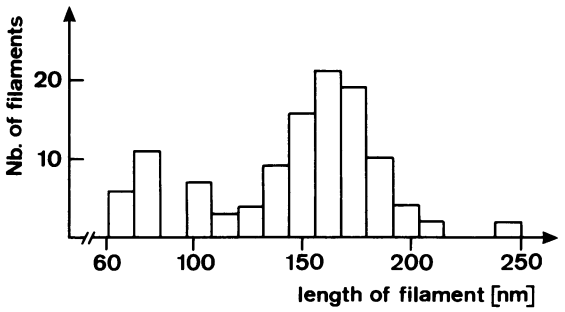

Fig. 10. Histogram of the length of 10 nm filaments appearing during dissociation of the globules exposed to a low salt buffer (0–10 mM NaCl). Data from all the measurable filaments of seven micrographs from three different preparations are presented here.

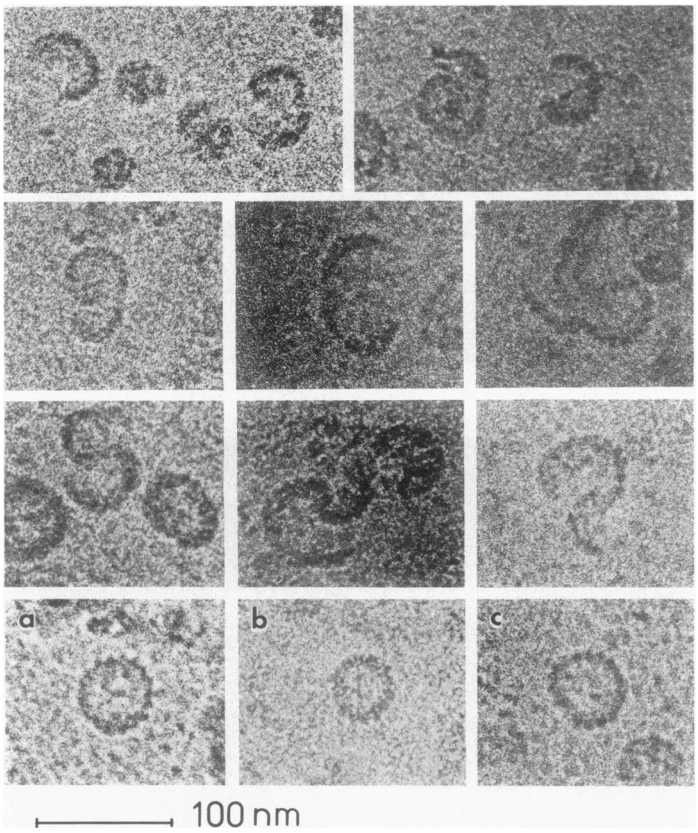

Fig. 11. Typical shape of the 10 nm filaments shortly after the minichromosome solution has been put into the low salt medium. **a**, **b** and **c** are roundish filaments on which rotational autocorrelation tests have been performed. Magnification: 180 000×.

or the fact that they are not in a horizontal plane. Nevertheless, a histogram of all the filaments longer than 50 nm, on several preparations, shows a marked peak at 165 ± 15 nm (Figure 10). The filaments of this peak have characteristic shapes: many form circles of about 50 nm diameter; others are 'C' or 'S'-shaped (Figure 11). The filaments are frequently striated along their length. The period of this striation can be measured directly on many filaments and is found to be 8 ± 1 nm. A correlation rotation test has been applied to the rings of the bottom line in Figure 11. As shown in Figure 12, the striation is reinforced for a displacement of 8 nm along the mid-line of the filament whereas other displacements lead to an attenuation.

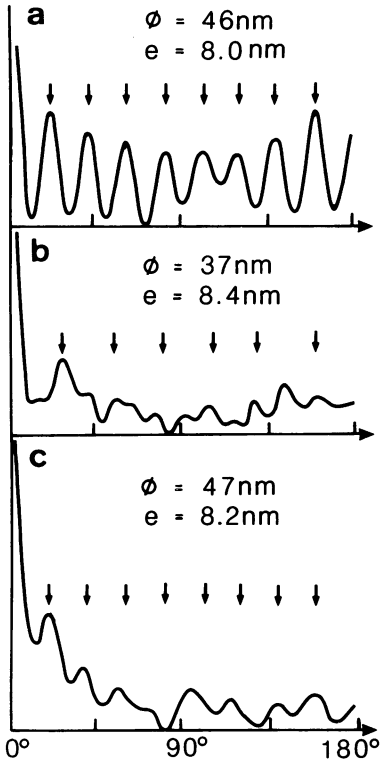

Fig. 12. Rotation correlation tests with the three filaments **a**, **b** and **c** on Figure 11. Each filament was digitized into 11–14 concentric circles for which the angular autocorrelation was calculated and averaged over the different circles. Φ is the diameter of the middle line of the filaments and **e** the corresponding displacement between the peaks (arrows). Calculations were made using the SEMPER programs (Saxton *et al.*, 1979).

As the 10 nm filaments become progressively dissociated, only groups of nucleosomes and portions of DNA filaments remain visible (Figure 13a). The aspect of the preparation is similar to that of chromatin isolated from chick erythrocytes (Figure 13b). Depending on their orientation, the nucleosomes appear as roundish bodies with a low-density central region and a diameter of about 10 nm (black arrows) or as wedge-shaped bodies of about 10 × 5 nm (white arrows). Capsomers of VP1 have a clearly smaller diameter (about 7 nm). They are recognizable in the background of some preparations or in partially disrupted viral capsids (Figure 13b, insert).

Discussion

Methodology

Cryo-electron microscopy of vitrified specimens is a new method. It requires some comments: the thin film vitrification method allows the preparation of biological specimens while preserving their aqueous and ionic environment. Evidence has been provided that vitrification has little effect on the structure of biological material (Adrian *et al.*, 1984; McDowall *et al.*, 1984). The possibility that specimens are partially dehydrated because water evaporates from the thin film solution, just before vitrification, has been tested by comparing the mass thickness before and after freeze-drying in the electron microscope. Under normal working conditions the amount of water and the salt concentration changes by less than 30% during preparation (Lepault *et al.*, 1983).

Conventional methods for preparing specimens for electron

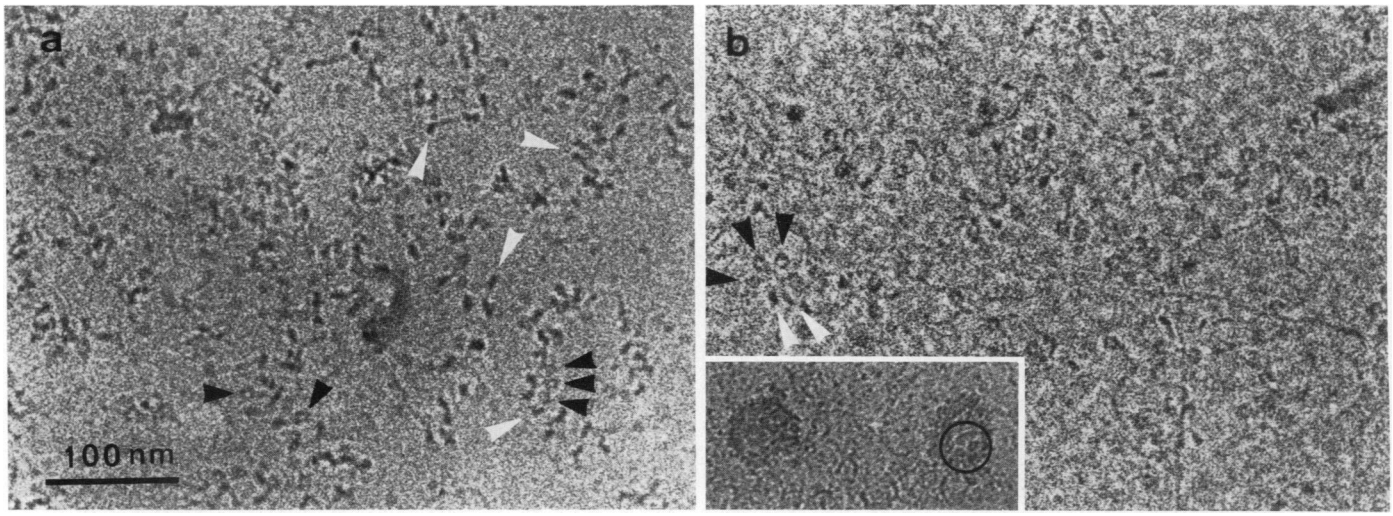

Fig. 13. (**a**) Open minichromosome after prolonged stay in low salt buffer (20 μg DNA/ml; < 5 mM NaCl). (**b**) Chicken erythrocyte chromatin in low salt buffer (350 μg DNA/ml; 2.5 mM NaCl). Black arrows: roundish nucleosomes. White arrows: wedge-shaped nucleosomes. Insert: partially disrupted viral capsids. A region where individual VP1 capsomers are visible is circled. Magnfication: 180 000×.

microscopy require several potentially damaging operations to be performed. These are, generally, chemical fixation, staining, dehydration and adsorption onto a supporting film. All these effects are avoided in the thin-film vitrification method, where the only preparation artefact results from interaction of particles with the liquid surface. Some examples of this effect have been described previously (Dubochet *et al.*, 1985).

The contrast of unstained vitrified specimens is sufficient for high resolution observations and it has the value expected from theory (Lepault and Pitt, 1984). One must, however, keep in mind that the visualization of unstained, vitrified structures—even those as large as whole globules—relies nearly entirely on phase contrast image formation, and not on amplitude contrast. The conditions for optimal use of phase contrast have been given in a previous publication (Adrian *et al.*, 1984). They require that unusually high under-focus is used.

The minichromosome

The complete molecular structure of the minichromosome cannot be deduced directly from the micrographs of vitrified specimens. Nevertheless, model building is possible on the hypothesis that the minichromosome is made of nucleosomes. The three levels of organization observed on the micrographs, namely: the nucleosomes, the 10 nm filaments, and the globules, can then be characterized in detail. The hypothesis that the nucleosome is the only building block of the minichromosome neglects, however, the possible role of the viral proteins VP1, 2 and 3. Further work is in progress to characterize their effects.

The nucleosome. SV40 and cellular nucleosomes have a similar DNA and histone content (Müller *et al.*, 1978; Shelton *et al.*, 1980) and the same appearance in conventional electron microscopy (references in: Tooze, 1982). One can therefore expect that the structure of the cellular nucleosome core particle which was schematically described as a wedge-shaped cylinder ~ 10 nm in diameter and 6 nm in height (Finche *et al.*, 1977; Dubochet and Noll, 1978; Richmond *et al.*, 1984) also describes the nucleosome of SV40. This expectation is supported by the observations of solutions of open minichromosome described here (Figure 13).

The 10 nm filament. This results from the stacking of nucleosomes, or in other words, the top-to-bottom superposition of the cylindrical nucleosomes. A schematic drawing is shown in Figure 14b. Other geometry, as for example the side-by-side juxtaposition of cylindrical nucleosomes which would result in a beaded structure with an approximately 10 nm repeat, are

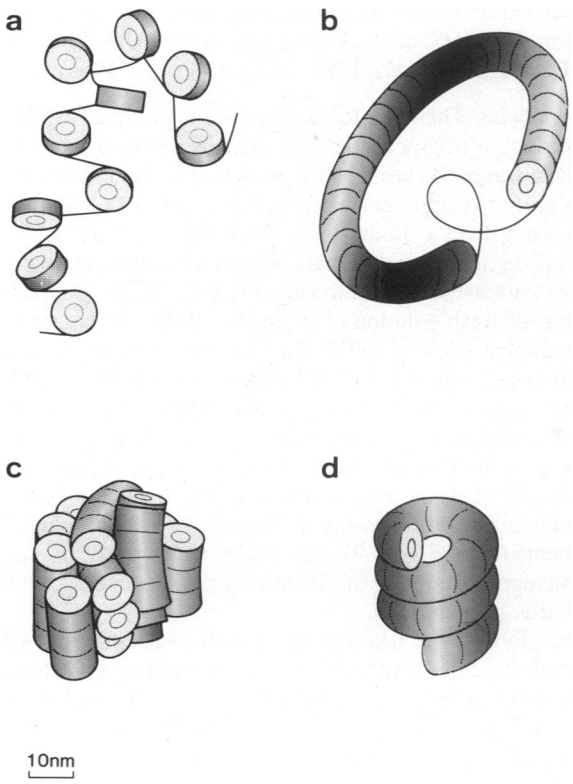

Fig. 14. Schematic drawing of the three condensation levels of the minichromosome. (**a**) Open minichromosome formed by nucleosomes bounded by flexible DNA linkers. (**b**) 10 nm filament formed by the stacking of nucleosomes. A nucleosome-free DNA linker has been drawn to close the loop. (**c**) and (**d**) Two possible globule structures. The DNA linkers have been omitted. In (**c**) the globule is formed by close packing of small fragments of 10 nm filaments from two minichromosomes. This model is suggested by the second globule of Figure 8b. In (**d**) the 10 nm filament of one minichromosome is rolled into a solenoid. This model is suggested by globules marked by black arrows in Figure 7a.

incompatible with the relatively smooth structure of the observed filament. It is reasonable to assume that each of the ~165 nm-long filaments are formed by the 20–25 nucleosomes of one minichromosome with each nucleosome therefore accounting for approximately 7 nm of the length of the filament. This value is close to the observed 8 nm transverse striation. It is, however, larger than the ~6 nm thickness of individual nucleosome core particles. The difference can be accounted for by a combination of the ~60 bp of linker DNA and by the presence of histone H1, non-histone proteins and viral-coded proteins which are associated with the SV40 minichromosomes. We note also the striking similarity between the 10 nm filaments observed here and the arches obtained by *in vitro* association of isolated nucleosome cores or rows of nucleosome cores found in some crystals (Finch *et al.*, 1977; Dubochet and Noll, 1978).

The fact that some of the 10 nm filaments do not form closed loops (see for example, the first three lines in Figure 11) does not mean that the DNA of the minichromosome is broken. In fact, agarose gel electrophoresis of the deproteinized DNA shows that the majority of the DNA molecules are still superhelical in the solution used for electron microscopy. A region of nude DNA could exist in many filaments, either because they are partially dissociated or as a result of the nucleosome-free gap, known to exist in 20–25% of the minichromosomes (Jakobovits *et al.*, 1980; Saragosti *et al.*, 1980; Jongstra *et al.*, 1984).

The Globules. These are formed by the compact packing of 10 nm filament(s) or fragments thereof. In many cases, groups of 10 nm filament fragments are directly recognizable in the globules. This is most clearly apparent when straight portions of filaments are seen along their cylinder axis. They then have the same roundish appearance as individual nucleosomes, although with much higher contrast. The 10 nm ring observed in the optical diffractogram of fresh solution of globules, further demonstrates that the compact packing of 10 nm filaments is a major structural feature observed in SV40 minichromosome solution. It should be stressed that the 10 nm ring, and therefore the close packing of 10 nm filaments is characteristic for fresh high-salt preparations. It is the first structural feature to disappear upon dilution in low salt or when the solution is aging. Images in which only individual nucleosomes (as in Figure 13) or individual 10 nm filaments (as in Figure 9) are visible, never result in an optical diffractogram showing the 10 nm ring. The same is true for entire virus preparations.

The globules are heterogeneous with respect to both size and internal structure. Although mass determination is difficult in phase contrast images, it is clear that the various globules shown (e.g. in Figures 3a, 7b and 8) are formed by different amounts of material. The size distribution of the globules selected for their circular appearance shows at least two populations: the major peak corresponds to a diameter around 30 nm and a spherical volume of 14×10^3 nm^3. This volume is compatible with that of a single hydrated minichromosome (mol. wt $\sim 6 \times 10^6$ daltons). The second peak at 37 nm could correspond to two minichromosomes packed at the same density. The shoulder towards the larger diameter in the distribution could correspond to globules formed by a still larger number of minichromosomes. Those particles around 20 nm are too small to contain a complete minichromosome. They are probably partially dissociated.

The globules are also heterogeneous with regard to their internal structure. The close packing of straight fragments of 10 nm filaments is a characteristic feature which has been described above. However, the extension of this feature to a whole globule would result in a bundle of parallel 10 nm filament fragments. This simple structure is not observed, with the possible exception of some of the smallest particles (Figure 8a). In fact, most globules are less ordered. The origin of the disorder probably lies in the heterogeneity of the length of the 10 nm filament fragments, their curvature and/or their non-parallelism. Heterogeneity in protein composition could also play a role. A possible model, suggested by the second globule of Figure 8b is shown in Figure 14c.

Other globules seem to be organized differently. This is, for example, the case for the small perforated cylinders seen in Figure 7a. Their shape and size suggest a helical arrangement of a 10 nm filament. Assuming that each nucleosome occupies 8 nm along the central line of the filament, this suggests that there are seven or eight nucleosomes per turn or about three turns for one minichromosome. A possible model of this conformation, resembling the classical solenoid (Thoma *et al.*, 1979) is represented in Figure 14d. The small striated circles shown in Figure 8c could be formed by one turn of 10 nm filaments wrapped around another short portion of filament.

We stress that the models presented in Figure 14 are not meant to be accurate descriptions of the structures of the minichromosomes. On the contrary, they serve to illustrate that one single model of a globule cannot account for the observed facts and to suggest how many more conformations could equally well be envisaged.

The fusion of the globules into an apparently homogeneous 'sea' of closely packed 10 nm filaments, as exemplified in Figure 6, is another aspect of the non-specificity of minichromosome condensation. The phenomenon of particle concentration, at the edge of the thinnest regions of the liquid film, just prior to vitrification, is frequent for every specimen prepared by this method. However, among all the specimens we have observed, including many kinds of nucleo-protein aggregates, such as ribosomes, or the delicate nuclear core of some viruses, only the minichromosome globules and other forms of chromatin (report in preparation) lose their apparent structure during the condensation process. This suggests that the globular shape of the minichromosome is not an intrinsic property but only the consequence of its isolation in the dilute suspension.

The Liquid Drop Model

In view of the above observations, the condensed form of minichromosomes can be described by the liquid drop model. This model applies to the minichromosomes in the 50–130 mM salt buffer. It states that (i) the nucleosomes tend to stack specifically on each other, thus forming the 10 nm filament, and (ii) the 10 nm filaments tend towards lateral aggregation. One way to maximize both of these interactions is to fold the continuous 10 nm filament on itself into a solenoid (Figure 14d). This solution requires, however, that the 10 nm filament adopts a small radius of curvature which is probably unfavourable. A compromise seems to involve breakage of the 10 nm filament into several fragments (without, of course, breaking the DNA molecule itself). The model assumes that the fragments are relatively independent, which requires that the DNA linker between nucleosomes is flexible. They may therefore aggregate into various conformations. The number of possible conformations becomes very large when it is considered that one globule may contain more than one minichromosome. The model implies that the various conformations of the minichromosomes are all accessible within the statistical fluctuation taking place during synthesis and preparation. This implies, by definition, that the globules

have the structure of a liquid. In other words, the model states that the 10 nm filament fragments are sufficiently independent from each other as to interact in a way analogous to the molecules of a liquid. The globules are then seen as insoluble droplets of 10 nm filament fragments floating in liquid water. One could argue that the various structures of the globules are the result of a heterogeneity existing at some early stage of synthesis or isolation of the minichromosome but that they are rigid in the purified solution. This is probably not the case and the observation that the globules lose their identity when they are put in close contact suggests that they are still mobile in purified solution. In other words, the liquid droplets of minichromosome are not vitrified.

Two lines of evidence speak in favour of the minichromosome of SV40 as a relevant model for native cellular chromatin. On the one hand, both have the same cellular origin and contain the same major biochemical components. The size of the minichromosome can be compared to individual replicons or to some of the hypothesized chromosome loops (Mirkovitch *et al.*, 1984). On the other hand, the minichromosome can be extracted, purified and prepared for electron microscopy while being kept in a physiological ionic environment. This is in contrast with cellular chromatin preparations which involve, at some stage, a passage at low ionic strength to disperse the chromatin fragments. It may be that some of the fundamental properties of the native chromatin are modified during this process. It must however be kept in mind that the minichromosome also contains virus encoded proteins. They could play a structural role which has not been considered here.

Extending the conclusions on the minichromosome to the native cellular chromatin implies that the latter is also in the liquid state. This hypothesis has deep implications. It can be understood as a statement on 'order management'. Obviously, there is a large amount of order in chromatin. Its various functions, which are precisely controlled in time and space, imply some form of structural order. We also know that chromatin consists of a linear array of particles (nucleosomes, 10 nm filament fragments or similar) distributed along one very long, continuous, DNA molecule. This reduces accordingly the freedom of the particles to occupy any position in space. Evidence for a scaffold also suggests the existence of a higher lever of structural organization and another degree of freedom reduction (Mirkovitch *et al.*, 1984).

Order — and disorder — is a property reflected in the structure of a solid as well as of a liquid. In a solid, order is expressd by a precise geometrical relationship between neighbouring particles. Disorder is then introduced in terms of a defect: some of the particles do not obey the relationship. A crystal is an example of a solid and a polycrystalline substance an example of a disordered solid. Many viruses are also solids, as would be a solenoid of nucleosomes. The type of organization found in a liquid is fundamentally different; the disorder is uniformly distributed over all particles. Thus, although there is still a geometrical relationship between neighbours, it is not sufficiently precise to force one given conformation. One major consequence is that the structure of a liquid can only be described in terms of interactions between many particles. Another is that liquids are mobile.

The liquid chromatin model implies that the conformation of neighbouring 10 nm filaments is not unique and varies with time. This does not mean that structures such as, for example, solenoids do not exist, but it implies that they can only be transient and randomly formed. The model also implies that local rearrangements can be made without long-range perturbation. This suggests, for example, that external molecules could easily diffuse through the liquid chromatin without need for global rearrangements.

In order to test the hypothesis of the liquid cellular chromatin, it is necessary that the work presented here is pursued beyond the SV40 minichromosome. Many questions raised by the hypothetical properties of the 10 nm filament must also be addressed. In particular, the structures and the forces involved in its remarkable flexibility which allow it to be either straight or to have a radius of curvature as small as 9 nm, must be understood. In this context, the possibility of a hinge built inside the nucleosome, as suggested in previous work (Dubochet and Noll, 1978), is still appealing. Finally, understanding the detailed structure, dynamics and function of chromatin in terms of a liquid formed from connected, filamentous particles, promises to be a formidable task. It may be, however, that the science of liquid crystals and of polymer gels has already brought us a long way towards this goal (Livolant, 1984).

Materials and methods

CV_1 cells were infected with SV40 (strain 777) and labelled with ^3H thymidine as described previously (Bellard *et al.*, 1976). Extraction and purification of the minichromosomes was carried out 40 h after infection in the presence of 0.13M NaCl according to the procedure of Varshavsky *et al.* (1977a). After sucrose gradient fractionation, the 75S peak was concentrated by centrifugation through a 30% sucrose cushion. The pellet was resuspended in 20 μl of 130 mM NaCl, 0.1 mM EDTA, 2 mM DTT, 0.2 mM PMSF, 10 mM TEA at pH 7.3 (high salt buffer) or, on some occasions, in the same buffer containing 50 mM NaCl. The concentration of minichromosome was adjusted for electron microscopy by dilution in the high salt buffer just prior to specimen preparation. The low-salt experiments were made by dilution in pure water or in the low-salt buffer, similar to the high-salt buffer but containing 10 mM NaCl instead. Most preparations were controlled by protein and DNA gel electrophoresis as described in Weiss *et al.* (1985). Chicken erythrocyte chromatin was prepared as described previously (Noll *et al.*, 1975). SV40 viruses were prepared and purified five days after infection according to Moyne and Harper (1982).

The method for specimen preparation and electron microscopical observation has been described previously (Adrian *et al.*, 1984; Dubochet *et al.*, 1982). A drop of the minichromosome solution at a concentration of 10−1000 μg/ml DNA was put on a bare 200 mesh copper grid or on a hydrophilic perforated carbon film, with an average hole diameter of 4μm. Most of the liquid was removed, either by firmly pressing a blotting paper towards the grid or by suction with a pipette. The grid was then immediately plunged into liquid ethane cooled by liquid nitrogen. It was then inserted, under liquid nitrogen, into the cryo-specimen holder PW6591/100 (Philips, Eindhoven, The Netherlands) and introduced into a Philips 400 electron microsocpe, equipped with a special anti-contaminator (Homo *et al.*, 1984). Observations were made at specimen temperatures around 100 K with 80 kV electrons. Images were underfocussed by 2−8 μm. For each micrograph presented here the first zero of the transfer function corresponds to a dimension smaller than any relevant structural feature observed. Electron optical contrast inversion is therefore excluded. Micrographs were recorded at magnifications of 20−30 thousand times on Kodak SO-163 film, developed 12′ in D-19, full strength. The electron irradiation was always minimized, in particular by using the low dose unit PW6587/01. Magnification was checked with a cross grating replica.

Acknowledgements

This work is dedicated to E.Kellenberger in friendship and respect. We thank E.Regnier and E.Weiss for help with the isolation of the minichromosome, Dr M.Vega for a gift of avian chromatin, Dr R.Vogel for help with the correlation rotation test, Drs P.G.De Gennes and H.Ludwig for valuable discussions, Drs M.F.Trendelenburg and J.M.Smith for their critical reading of the manuscript, and Ms C.Barber for her patience in dealing with authors and computer.

References

Adrian,M., Dubochet,J., Lepault,J., McDowall,A.W. (1984) *Nature*, **308**, 32–36.

Bellard,M., Oudet,P., Germond,J.E. and Chambon,P. (1976) *Eur. J. Biochem.*, **70**, 543–553.

Dubochet,J. and Noll,M. (1978) *Science*, **202**, 280–286.

Dubochet,J., Ducomun,M., Zollinger,M. and Kellenberger,E. (1971) *J. Ultrastruct. Res.*, **35**, 147–167.

Dubochet,J., Lepault,J., Freeman,R., Berriman,J.A. and Homo,J.-C. (1982) *J. Microsc.*, **128**, 219–237.

Dubochet,J., Adrian,M., Lepault,J. and McDowall,A.W. (1985) *Trends in Biochem. Sci.*, **10**, 143–146.

Finch,J.T., Lutter, L.C., Rhodes,D., Brown,R.S., Rushten,B., Levitt,M. and Klug,A. (1977) *Nature*, **269**, 29–36.

Griffiths,J.D. (1975) *Science*, **187**, 1202–1203.

Homo,J.-C., Booy,F., Labouesse,P. and Lepault,J. (1984) *J. Microsc.*, **136**, 337–340.

Jakobovits,E.B., Bratosin,S. and Aloi,Y. (1980) *Nature*, **285**, 263–265.

Jongstra,J., Reudelhuber,T., Oudet,P., Benoist,C., Chae,C.B., Jeltsch,J.M., Mathis,D.J. and Chambon,P. (1984) *Nature*, **307**, 708–714.

Keller,W., Müller,U., Eicken,I., Wendel,I. and Zentgraf,H. (1978) *Cold Spring Harbor Symp. Quant. Biol.*, **42**, 227–244.

Lepault,J. and Pitt,T. (1984) *EMBO J.*, **3**, 101–105.

Lepault,J., Booy,F.P. and Dubochet,J. (1983) *J. Microsc.*, **129**, 89–102.

Livolant,F. (1984) *Eur. J. Cell Biol.*, **33**, 300–311.

McDowall,A.W., Hofmann,W., Lepault,J., Adrian,M. and Dubochet,J. (1984) *J. Mol. Biol.*, **178**, 105-111.

Mirkovitch,J., Mirault,M.E. and Laemmli,U.K. (1984) *Cell*, **39**, 223–232.

Moyne,G. and Harper,F. (1982) *Cell*, **30**, 123–130.

Müller,U., Zentgraf,H., Eicken,I. and Keller,W. (1978) *Science*, **201**, 406–415.

Noll,M., Thomas,J.D. and Kornberg,R.D. (1975) *Science*, **187**, 1203–1206.

Oudet,P., Gross-Bellard,M. and Chambon,P. (1975) *Cell*, **4**, 281-300.

Richmond,T.J., Finch,J.T., Rushten,B., Rhodes,D. and Klug,A. (1984) *Nature*, **311**, 532-537.

Saragosti,S., Moyne,G. and Yaniv,M. (1980) *Cell*, **20**, 65–73.

Saxton,W.O., Pitt,T.J. and Horner,M. (1979) *Ultramicroscopy*, **4**, 343–354.

Shelton,E.R., Wasserman,P.M. and De Pamphilis,M.L. (1980) *J. Biol. Chem.*, **255**, 771–782.

Thoma,F., Koller,Th. and Klug,A. (1979) *J. Cell. Biol.*, **83**, 403–427.

Tooze,J. (1982) *DNA Tumor Viruses*. Cold Spring Harbor Laboratory Press, Cold Spring Harbor, NY.

Varshavsky,A.J., Nedospasov,S.A., Schomatchenko,V.V., Bakayev,V.V., Chamakov,P.M. and Georgiev,G.P. (1977) *Nucleic Acids Res.*, **4**, 3303–3324.

Varshavsky,A.J., Bakayev,V.V., Nedospasov,S.A. and Georgiev,G.P. (1978) *Cold Spring Harbor Symp. Quant. Biol.*, **42**, 457–474.

Weiss,E., Dipankar,G., Schultz,P. and Oudet,P. (1985) *Chromosoma*, in press.

Received on 28 May 1985; revised on 2 January 1986